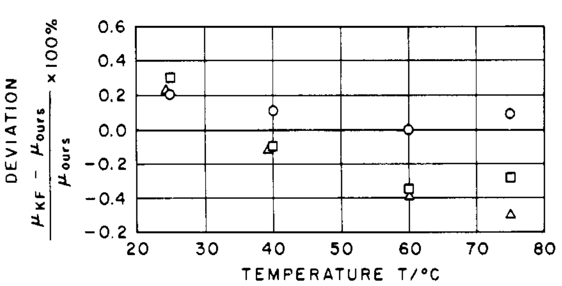

Figure 4. Deviation of the viscosity measurements of ref *13* from the calculated values via eq 10–14: (○) $c = 0.3330$ *m*; (□) $c = 0.2356$ *m*; (△) $c = 0.4712$ *m*.

The coefficients f_{ij} and g_{ij} which appear in eq 11 and 13, respectively, were calculated from the measurements presented earlier. The resulting coefficients are seen listed in Tables XIII and XIV for Na_2SO_4 solutions and Tables XV and XVI for K_2SO_4 solutions, respectively.

Figures 2 and 3 depict the deviations of the experimental results from the correlations for Na_2SO_4 and K_2SO_4, respectively. The correlations reproduce the experimental results with a maximum deviation of 0.9% for Na_2SO_4 solutions and 0.7% for K_2SO_4 solutions. The standard deviation is 0.4% for the Na_2SO_4 as well as the K_2SO_4 solutions, which is well within the estimated accuracy of the experimental data.

The only measurements of viscosity available for comparison are those by Korosi and Fabuss (*13*) for aqueous Na_2SO_4 solutions. Figure 4 depicts the deviation of these measurements from the correlations presented here. The deviations are within ±0.5% with a standard deviation of 0.26%, which is within the quoted accuracy of the measurements.

Acknowledgment

We express our thanks to Mr. Roger Paul for maintaining the experimental installation.

Literature Cited

(1) Correia, R. J.; Kestin, J.; Khalifa, H. E. *Ber. Bunsenges. Phys. Chem.* **1979**, *83*, 20.
(2) Correia, R. J.; Kestin J.; Khalifa, H. E. *J. Chem. Eng. Data*, in press.
(3) Grimes, C. E.; Kestin, J.; Khalifa, H. E. *J. Chem. Eng. Data* **1979**, *24*, 121.
(4) Kestin, J.; Khalifa, H. E. *Appl. Sci. Res.* **1976**, *32*, 483.
(5) Kell, G. S.; Whalley, E. *J. Chem. Phys.* **1975**, *62*, 3496.
(6) Kestin, J.; Khalifa, H. E.; Abe, Y.; Grimes, C. E.; Sookiazian, H.; Wakeham, W. A. *J. Chem. Eng. Data* **1978**, *23*, 328.
(7) Kestin, J.; Khalifa, H. E.; Ro, S. T.; Wakeham, W. A. *J. Chem. Eng. Data* **1977**, *22*, 207.
(8) Kestin, J.; Khalifa, H. E.; Sookiazian, H.; Wakeham, W. A. *Ber. Bunsenges. Phys. Chem.* **1978**, *82*, 180.
(9) Kestin, J.; Leidenfrost, W.; Liu, C. V. *Z. Angew. Math. Phys.* **1959**, *10*, 558.
(10) Kestin, J.; Moszynski, J. R. *Trans. ASME* **1958**, *80*, 1009.
(11) Kestin, J.; Sokolov, M.; Wakeham, W. A. *J. Phys. Chem. Ref. Data* **1978**, *7*, 941.
(12) Kestin, J.; Wang, H. E. *J. Appl. Mech.* **1957**, *79*, 197.
(13) Korosi, B. M.; Fabuss, A. *J. Chem. Eng. Data* **1968**, *13*, 548.
(14) Potter, R. W., II; Brown, D. L. *Geol. Surv. Open-File Rep.* (*U.S.*), *No. 76-255*, 1976.
(15) Potter, R. W. II; Brown, D. L. *Geol. Surv. Open-File Rep.* (*U.S.*), *No. 76-501*, 1976.
(16) Potter, R. W., II; Shaw, D. K.; Haas, J. L., Jr. *Geol. Surv. Bull.* (*U.S.*) **1975**, *No. 1417*.

Received for review May 19, 1980. Accepted July 30, 1980. Financial support was provided by the U.S. Geological Survey (Grant 14-08-0001-G-342). One of the authors, R. J. Correia, was also in receipt of a National Science Foundation Graduate Traineeship made available through Brown University.

Solubility of Solids in Supercritical Carbon Dioxide and Ethylene

Ronald T. Kurnik, Samuel J. Holla, and Robert C. Reid*

Department of Chemical Engineering, Massachusetts Institute of Technology, Cambridge, Massachusetts 02139

Solubility data were obtained for five different solids in both supercritical carbon dioxide and supercritical ethylene. A one-pass flow system was used to measure the equilibrium solubilities. The range in temperatures covered was 308–338 K and the range in pressures was roughly 80–280 bar.

Over the past few years, significant interest has been expressed in a separation concept wherein a condensed phase (liquid or solid) is contacted with a fluid phase that is supercritical both in the temperature and pressure sense. An often-quoted example is the German patent to remove, selectively, caffeine from green coffee beans by using supercritical carbon dioxide (*24*). Other examples would include deasphalting heavy residual oils with supercritical propane (*19*) and removing adsorbed materials from activated carbon with supercritical carbon dioxide (*8*, *9*). Supercritical water has been explored as a solvent medium to carry out chemical reactions or biological degradations without char formation (*1*, *7*).

In all of these instances, the dissolution effect appears to be related primarily to the nonideality of the supercritical fluid phase which leads to solvent behavior more representative of a liquid phase—at temperatures above what could have been attained if only a liquid had been used. Also, because of the high density of the supercritical solvent, process volumes are reduced (but the high pressure increases equipment costs) and transport properties are intermediate in value between those of a gas and a liquid; i.e., diffusion coefficients are much higher than for typical liquids.

Table I. References with Solubility of Solids in Supercritical Fluids

solid	solvent	*T*, K	*P*, bar	ref
hexachloroethane	ethylene	289.5–296.5	1–170	*22*
naphthalene	ethylene	289.5–296.5	1–170	*22*
hexachloroethane and naphthalene	ethylene	289.5–296.5	1–170	*22*
quartz	water	653–698	300–500	*23*
quartz	water	423–873	1–1000	*5*
naphthalene	ethylene	285–318	50–300	*20*
naphthalene	carbon dioxide	308–328	60–330	*20*
naphthalene	ethylene	285–308	40–100	*3*
phenanthrene	ethylene	313	138–551	*4*
phenanthrene	ethane	313	138–551	*4*
phenanthrene	carbon dioxide	313	138–551	*4*
phenanthrene	methane	313	138–551	*4*
diphenylamine	carbon dioxide	305–310	50–225	*21*

In view of the interest expressed in this technology, it is surprising that so few data exist to illustrate quantitatively the solvent effect. In Table I, we summarize those references known to us that provide equilibrium solubility data. Not shown in this table are a number of other references which relate only

0021-9568/81/1726-0047$01.00/0

to the pressure–temperature behavior of high-pressure systems wherein a solid (or liquid) phase is in equilibrium with a gas (fluid).

Knowing the $P-T$ behavior of a binary system is, however, very necessary as only those systems with critical end points are viable for supercritical extraction. Rowlinson (*16*) discusses this problem, and Modell et al. (*10*) have estimated the critical end points for the systems carbon dioxide–naphthalene and ethylene–naphthalene by using an equation-of-state approach. Normally, however, if the condensed phase is solid and has a melting point significantly above the critical point of the solvent, then supercritical extraction is a suitable method for separation.

In this paper we present new experimental equilibrium solubilities for five solid systems by using both supercritical carbon dioxide and ethylene. It is also shown that these data may be well correlated by using thermodynamic relationships and an equation of state.

Thermodynamic Relationships

The thermodynamics applicable to relate the equilibrium mole fraction of a solute dissolved in a high-pressure gas (fluid) have been treated earlier by Prausnitz (*13*, *14*). The results may be written in a deceptively simple form. With 1 representing the solute which both is present as a pure solid and is dissolved in the fluid phase

$$y_1 = (P_{\mathrm{vp}_1}/P)(1/\phi_1)\exp[(V_1/RT)(P - P_{\mathrm{vp}_1})] \qquad (1)$$

with y_1 the fluid-phase mole fraction of 1.

In eq 1 it has been assumed that: (a) the fluid-phase component does not dissolve in the solid, (b) the molar volume of the solid is independent of pressure, and (c) the fugacity coefficient of pure vapor 1 at T and P_{vp_1} is unity. In most instances, these three assumptions are appropriate.

The only term on the right-hand side of eq 1 which reflects the fact that the fluid phase is a mixture is the fugacity coefficient of component 1, ϕ_1. Accurate estimates of this variable are necessary to determine y_1. ϕ_1 can be found from an applicable mixture equation of state using well-known thermodynamics (*6*). We have employed both the Soave (*18*) and the Peng–Robinson (*12*) modifications of the Redlich–Kwong equation of state (*15*). Both provide equally good estimates of ϕ. Only the Peng–Robinson form is illustrated here.

$$\ln \phi_i = \frac{b_i}{b}(Z - 1) - \ln (Z - B) - \frac{A}{2B2^{1/2}}\left\{2\sum_j (1 - k_{ij})\frac{[a_i(T)a_j(T)]^{1/2}}{a(T)}y_j - \frac{b_i}{b}\right\} \ln \left(\frac{Z + 2.414B}{Z - 0.414B}\right) \qquad (2)$$

In this equation Z is the compressibility factor of the gas mixture and is found from the original equation of state

$$Z^3 - (1 - B)Z^2 + (A - 3B^2 - 2B)Z - (AB - B^2 - B^3) = 0 \qquad (3)$$

To calculate ϕ, or Z, pure component parameters a_i and b_i are found from eq 4 and 6 using critical properties and acentric factors.

$$a_i = \Omega_a \frac{R^2 T_{c_i}^{\,2}}{P_{c_i}} [1 + \kappa_i(1 - T_{r_i}^{\,1/2})]^2 \qquad (4)$$

where

$$\kappa_i = 0.37464 + 1.54226\omega_i - 0.26992\omega_i^{\,2} \qquad (5)$$

$$b_i = \Omega_b R T_{c_i}/P_{c_i} \qquad (6)$$

Table II. Solid Properties

solid	mp,[a] K	T, K	vapor press., Pa	vapor press., ref	supplier, purity
2,3-dimethylnaphthalene	376	308	1.27	*11*	Aldrich, 99%
		318	3.49		
		328	9.01		
2,6-dimethylnaphthalene	382	308	1.22	*11*	Aldrich, 99%
		318	3.45		
		328	9.13		
phenanthrene	374	318	0.155	*2*	Eastman Kodak, 98%
		328	0.423		
		338	1.09		
benzoic acid	396	318	0.780	*2*	Aldrich, 99%
		328	2.16		
		338	5.62		
hexachloroethane	460	308	154	*17*	Aldrich, 99%
		318	284		
		328	504		

[a] At 1 bar.

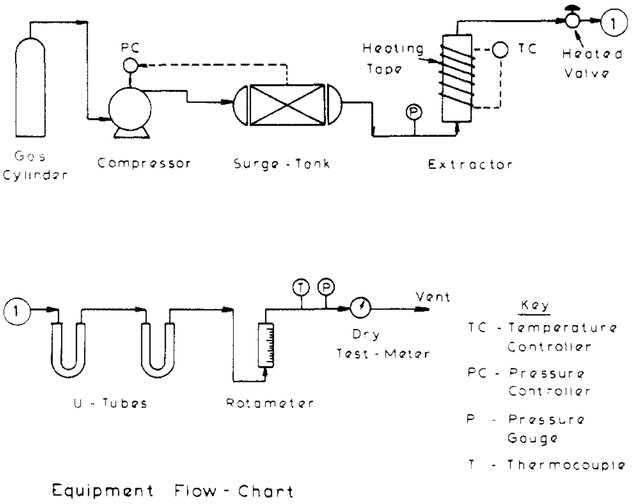

Figure 1. Equipment flow chart.

Mixing parameters a and b are related to the pure component terms a_i and b_i by eq 7 and 8. Variables A and B as used in

$$a = \sum_i \sum_j x_i x_j a_i^{1/2} a_j^{1/2}(1 - k_{ij}) \qquad (7)$$

$$b = \sum_i x_i b_i \qquad (8)$$

eq 2 and 3 are defined by eq 9 and 10. The interaction

$$A = aP/(R^2T^2) \qquad (9)$$

$$B = bP/(RT) \qquad (10)$$

parameter k_{ij} is characteristic of a binary pair (i and j) and is normally assumed to be independent of pressure, composition, or temperature. As will be seen later, however, we did find a weak temperature effect on k_{ij} for very nonideal fluid mixtures at high pressures.

Experimental Section

The solubilities of four relatively nonvolatile solids (2,3-dimethylnaphthalene, 2,6-dimethylnaphthalene, phenanthrene, and benzoic acid) were measured in both supercritical carbon dioxide and ethylene. In addition, hexachloroethane solubility was determined in supercritical carbon dioxide. In Table II we list the important physical properties of these pure solids. Temperatures ranged from 308 to 338 K and pressures from ~80 to 280 bar.

Experimental data were obtained with the flow system shown schematically in Figure 1. The feed gas (carbon dioxide or

Table III. Comparison of Test Data with Those of Tsekhanskaya (*20*) for CO_2-Naphthalene at 328 K

system press., bar	run time, min	10^3(volume of CO_2),[a] m^3	mass of naphthalene collected, g	10^2(mol fraction of naphthalene)	
				this work	Tsekhanskaya
125	20	10.00	0.75	1.40	1.42
162	10	5.00	0.79	2.92	3.00
197	10	5.00	1.10	4.01	3.99
253	8	4.00	1.06	4.79	4.85

[a] The pressure at the dry-test meter was 1.011 bar, and the temperature 295.4 K (except for the 253-bar test when it was 294.8 K).

ethylene) was compressed to the system pressure with an AMINCO single-stage compressor. Pressure fluctuations were dampened with an on-line surge tank fitted with a pressure controller at the outlet. Pressures were easily controlled to ±1 bar. The high-pressure fluid, at ambient temperature, was allowed to flow into a vertical extraction tube 1.8 cm in diameter and 30 cm long. By virtue of a low fluid flow rate, calculations and experimental temperature traverses showed that the fluid very rapidly attained the temperature in the extraction tube.

The extraction tube was packed with alternate layers of the test solid and quartz wool. It was wrapped with heating tape, and the temperature monitored with a thermocouple placed in the center of the tube. The vessel temperature could be controlled to ±0.5 K. Pressures in the extraction tube were measured with a calibrated Heise gauge mounted at the inlet. The pressure drop across the bed was negligible.

The supercritical extractant with dissolved solid passed from the extractor into a heated regulating valve and was subsequently expanded to 1 bar. The dissolved solids precipitated in a U-tube (at room temperature) following the valve. A second U-tube in the train was employed to insure trapping of all of the solid. Both tubes were packed with quartz wool at the outlet. In all cases over 99% of the solid was always trapped in the first U-tube.

The solute-free, low-pressure extractant-gas flow was measured by a rotameter (to insure steady flow) and by a calibrated Singer dry-test meter—at which point the stream temperature and pressure were also measured.

As the U-tubes were initially tared, the mass of precipitated solid was found by weighing the tubes after an experiment on a Mettler balance accurate to ±5 mg. With this value and the total extractant flow from the dry-test meter, the concentration of the solids in the supercritical fluid was readily determined. (In all cases, the amount of solute in the gas leaving the dry test meter was negligible.)

A number of experiments were conducted to insure that the technique would provide accurate and reliable equilibrium solubilities. The most important proof test was to run with the system naphthalene–carbon dioxide so as to compare the measured values of naphthalene solubility with those of Tsekhanskaya (*20*). In Table III we show the results for four runs at 328 K. When the equilibrium solubilities are compared with Tsekhanskaya's data, the average deviation is only 1.3%.

We also carried out tests for long times but separated the run into several periods. At the start of each period, new (tared) U-tubes were inserted and the previous tubes removed. No change in equilibrium concentration was noted when data from the different time periods were compared.

We also carried out repeat tests (for naphthalene–CO_2) in which we varied the position of the solid in the extractor; i.e., data were obtained with the solid distributed evenly in layers over the entire height (the usual mode), with the solid only in the lower half, and with solid only in the top half. Identical results were obtained for all tests at the same temperature and pressure. These results indicated that the extractor was isothermal and, also, that equilibrium was rapidly attained.

Table IV. CO_2-2,6-Dimethylnaphthalene Data

T = 308 K (k_{12} = 0.101)		T = 318 K (k_{12} = 0.0989)		T = 328 K (k_{12} = 0.100)	
P, bar	y	P, bar	y	P, bar	y
97	1.90×10^{-3}	98	7.57×10^{-4}	96	3.05×10^{-4}
145	2.96×10^{-3}	146	3.94×10^{-3}	146	4.31×10^{-3}
195	3.83×10^{-3}	194	5.09×10^{-3}	195	6.15×10^{-3}
245	4.01×10^{-3}	244	6.27×10^{-3}	246	7.99×10^{-3}
280	4.47×10^{-3}	280	6.77×10^{-3}	280	9.21×10^{-3}

Table V. CO_2-2,3-Dimethylnaphthalene Data

T = 308 K (k = 0.0996)		T = 318 K (k_{12} = 0.102)		T = 328 K (k_{12} = 0.106)	
P, bar	y	P, bar	y	P, bar	y
99	2.20×10^{-3}	99	1.28×10^{-3}	99	3.40×10^{-4}
143	4.40×10^{-3}	145	4.79×10^{-3}	146	4.45×10^{-3}
194	5.41×10^{-3}	195	6.37×10^{-3}	197	7.14×10^{-3}
242	5.82×10^{-3}	242	6.88×10^{-3}	241	8.47×10^{-3}
280	6.43×10^{-3}	280	7.19×10^{-3}	280	9.01×10^{-3}

Table VI. C_2H_4-2,6-Dimethylnaphthalene Data

T = 308 K (k_{12} = 0.0225)		T = 318 K (k_{12} = 0.0200)		T = 328 K (k_{12} = 0.0166)	
P, bar	y	P, bar	y	P, bar	y
80	4.83×10^{-4}	78	1.88×10^{-4}	78	2.36×10^{-4}
120	2.35×10^{-3}	120	2.19×10^{-3}	120	2.20×10^{-3}
159	4.61×10^{-3}	160	5.56×10^{-3}	160	6.74×10^{-3}
200	6.95×10^{-3}	200	9.08×10^{-3}	200	1.30×10^{-2}
240	9.27×10^{-3}	240	1.38×10^{-2}	240	2.00×10^{-2}
280	1.09×10^{-2}	280	1.71×10^{-2}	280	2.75×10^{-2}

Table VII. C_2H_4-2,3-Dimethylnaphthalene Data

T = 308 K (k_{12} = 0.0246)		T = 318 K (k_{12} = 0.0208)		T = 328 K (k_{12} = 0.0147)	
P, bar	y	P, bar	y	P, bar	y
77	3.13×10^{-4}	80	3.66×10^{-4}	80	3.00×10^{-4}
120	2.58×10^{-3}	120	2.58×10^{-3}	122	3.17×10^{-3}
159	6.02×10^{-3}	160	7.18×10^{-3}	160	8.78×10^{-3}
200	9.65×10^{-3}	200	1.21×10^{-2}	200	1.89×10^{-2}
240	1.26×10^{-2}	240	1.83×10^{-2}	240	3.21×10^{-2}
280	1.50×10^{-2}	280	2.41×10^{-2}	280	5.24×10^{-2}

Table VIII. CO_2-Phenanthrene Data

T = 318 K (k_{12} = 0.113)		T = 328 K (k_{12} = 0.108)		T = 338 K (k_{12} = 0.106)	
P, bar	y	P, bar	y	P, bar	y
120	8.49×10^{-4}	120	4.65×10^{-4}	120	3.28×10^{-4}
160	1.40×10^{-3}	160	1.51×10^{-3}	160	1.18×10^{-3}
200	1.70×10^{-3}	200	2.14×10^{-3}	200	2.37×10^{-3}
240	2.23×10^{-3}	240	2.79×10^{-3}	240	3.28×10^{-3}
280	2.28×10^{-3}	280	3.19×10^{-3}	280	3.84×10^{-3}

Tests were also run in which the flow rates was varied from 0.036 to 0.13 standard m^3/h. No effect was noted in the outlet concentration of naphthalene, and this reinforces our conclusion that equilibrium was rapidly achieved.

Results and Discussion

The equilibrium solubilities found in this work are shown in Tables IV–XII. In addition to noting the mole fraction of the solutes in the supercritical fluid, we also show the solute–solvent interaction parameter determined from the data and the Peng–Robinson equation of state.

Table IX. C_2H_4-Phenanthrene Data

$T = 318$ K ($k_{12} = 0.0459$)		$T = 328$ K ($k_{12} = 0.0355$)		$T = 338$ K ($k_{12} = 0.0318$)	
P, bar	y	P, bar	y	P, bar	y
120	8.16×10^{-4}	120	7.38×10^{-4}	120	7.43×10^{-4}
160	1.74×10^{-3}	160	1.76×10^{-3}	160	1.84×10^{-3}
200	2.67×10^{-3}	200	3.33×10^{-3}	200	3.64×10^{-3}
240	3.70×10^{-3}	240	5.34×10^{-3}	240	6.38×10^{-3}
280	4.56×10^{-3}	280	8.29×10^{-3}	280	1.06×10^{-2}

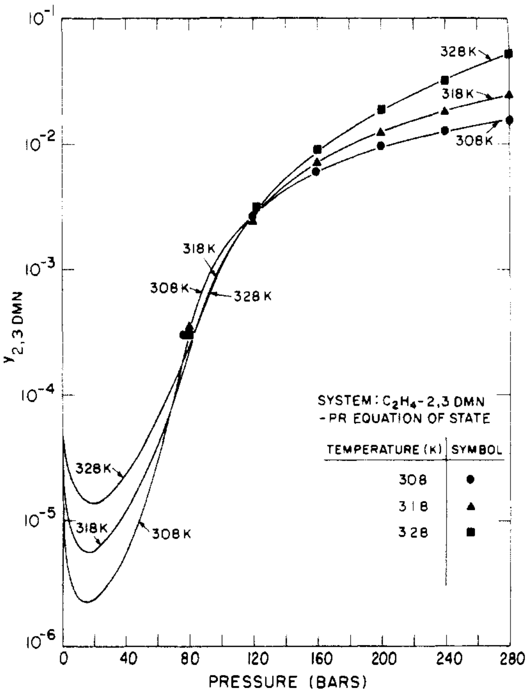

Figure 2. Solubility of 2,3-dimethylnaphthlene in ethylene.

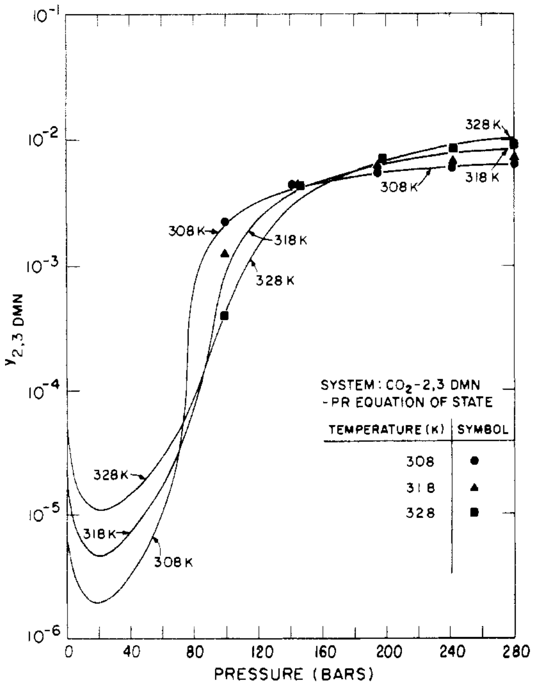

Figure 3. Solubility of 2,3-dimethylnaphthalene in carbon dioxide.

Table X. CO_2-Benzoic Acid Data

$T = 318$ K ($k_{12} = 0.00994$)		$T = 328$ K ($k_{12} = -0.00172$)		$T = 338$ K ($k_{12} = -0.0124$)	
P, bar	y	P, bar	y	P, bar	y
120	1.14×10^{-3}	120	4.90×10^{-4}	120	3.20×10^{-4}
160	2.37×10^{-3}	160	2.27×10^{-3}	160	1.72×10^{-3}
200	3.18×10^{-3}	200	3.86×10^{-3}	200	4.10×10^{-3}
240	4.21×10^{-3}	240	5.16×10^{-3}	240	6.95×10^{-3}
280	4.38×10^{-3}	280	7.34×10^{-3}	280	9.83×10^{-3}

Table XI. C_2H_4-Benzoic Acid Data

$T = 318$ K ($k_{12} = -0.0562$)		$T = 328$ K ($k_{12} = -0.0641$)		$T = 338$ K ($k_{12} = -0.0755$)	
P, bar	y	P, bar	y	P, bar	y
120	5.76×10^{-4}	120	5.48×10^{-4}	120	5.43×10^{-4}
160	1.35×10^{-3}	160	1.60×10^{-3}	160	1.92×10^{-3}
200	1.90×10^{-3}	200	2.61×10^{-3}	200	3.50×10^{-3}
240	2.90×10^{-3}	240	3.61×10^{-3}	240	4.93×10^{-3}
280	2.91×10^{-3}	280	4.08×10^{-3}	280	6.18×10^{-3}

Table XII. CO_2-Hexachloroethane Data

$T = 308$ K ($k_{12} = 0.129$)		$T = 318$ K ($k_{12} = 0.123$)		$T = 328$ K ($k_{12} = 0.116$)	
P, bar	y	P, bar	y	P, bar	y
99	1.45×10^{-2}	100	1.03×10^{-2}	97	3.79×10^{-3}
149	1.86×10^{-2}	148	2.39×10^{-2}	145	2.32×10^{-2}
199	1.96×10^{-2}	198	2.60×10^{-2}	195	3.89×10^{-2}
248	1.99×10^{-2}	247	2.78×10^{-2}	245	3.93×10^{-2}
280	1.80×10^{-2}	280	2.70×10^{-2}	280	3.89×10^{-2}

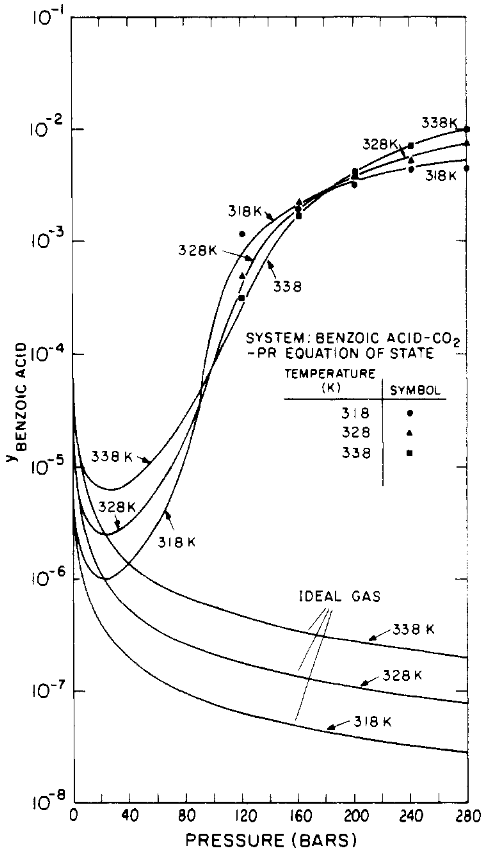

Figure 4. Solubility of benzoic acid in carbon dioxide (mole fractions are uncorrected for dimerization).

The data for the 2,3-dimethylnaphthalene test systems are shown in Figures 2 and 3. At comparable temperatures and pressures, ethylene normally is a much better solvent than CO_2, but, when comparisons are made at the same reduced conditions, then CO_2 is a more efficacious solvent.

The solid curves in Figures 2 and 3 represent the prediction of the equilibrium solubility using eq 1 and the interaction parameters in Tables V and VII. These k_{ij} values were found by using a nonlinear least-squares regression technique to give the best fit between theory and experiment.

In Figure 4, the experimental benzoic acid mole fractions in supercritical carbon dioxide are shown as a function of temperature and pressure. These data are also well correlated with the Peng–Robinson equation of state. Also shown in this figure are the calculated benzoic acid concentrations for cases where the vapor phase is assumed to behave as an ideal gas.

The ideal-gas assumption (ϕ_1 of eq 1 is unity) is valid only at very low pressures. At high pressures, an ideal-gas assumption grossly underestimates the actual concentration.

Acknowledgment

We thank the Computer Center, Massachusetts Institute of Technology, for the use of its facilities.

Glossary

a, b, A, B	variables in Peng–Robinson equation of state
k_{ij}	Peng–Robinson binary interaction parameter
P	pressure, bar
P_{vp}	vapor pressure, bar
R	gas constant
T	temperature, K
V	molar volume, cm^3/mol
y	fluid-phase mole fraction
Z	compressibility factor

Greek Letters

κ	parameter in Peng–Robinson equation of state
ϕ	fugacity coefficient
ω	acentric factor
Ω_a, Ω_b	constants in Peng–Robinson equation of state

Subscripts

1	solid component
2	fluid component
c	critical property
r	reduced property

Literature Cited

(1) Amin, S.; Reid, R. C.; Modell, M., paper presented at the Intersociety Conference on Environmental Systems, San Francisco, 1975.

(2) de Kruif, C. G.; van Ginkel, C. H. D.; Voogd, J., presented at the Quatrieme Conference Interactionale de Thermodynamique Chimique, 26 au 30, Montpellier, France, 1975.

(3) Diepen, G. A. M.; Scheffer, F. E. C. *J. Am. Chem. Soc.* **1948**, *70*, 4085.

(4) Eisenbeiss, J. San Antonio, TX, Aug 1964, Southwest Research Institute Final Report Contract No. DA 18-108-AMC-244(A).

(5) Jones, D.; Staehle, R., Ed. "High Temperature High Pressure Electro-Chemistry in Aqueous Solutions"; National Society of Corrosion Engineers, 1973; p 131.

(6) Modell, M.; Reid, R. C. "Thermodynamics and its Applications"; Prentice Hall: Englewood Cliffs, NJ, 1974; Chapter 8.

(7) Modell, M., paper presented at the Intersociety Conference on Environmental Systems, San Francisco, 1977.

(8) Modell, M.; Robey, R.; Krukonis, V.; deFilippi, R.; Oestreich, D., paper presented at the 87th National Meeting, AIChE, Boston, 1979.

(9) Modell, M.; deFilippi, R.; Krukonis, V., paper presented at the ACS meeting, Miami, Sept 1978.

(10) Modell, M.; Hong, G.; Helba, A., paper presented at the 72nd Annual Meeting, AIChE, Nov 1979.

(11) Osborn, A. G.; Douslin, D. R. *J. Chem. Eng. Data* **1975**, *20*, 229.

(12) Peng, D. Y.; Robinson, D. B. *Ind. Eng. Chem. Fundam.* **1976**, *15*, 59.

(13) Prausnitz, J. M. *NBS Tech. Note* (*U.S.*) **1965**, *316*.

(14) Prausnitz, J. M. "Molecular Thermodynamics of Fluid Phase Equilibria"; Prentice-Hall: Englewood Cliffs, NJ, 1969; Chapter 5.

(15) Redlich, O.; Kwong, J. N. S. *Chem. Rev.* **1949**, *44*, 233.

(16) Rowlinson, J. S. "Liquids and Liquid Mixtures", 2nd ed.; Butterworths: London, 1969.

(17) Sax, N. I. "Dangerous Properties of Industrial Materials", 5th ed.; Van Nostrand-Reinhold: Princeton, NJ, 1979; p 718.

(18) Soave, G. *Chem. Eng. Sci.* **1972**, *27*, 1197.

(19) Solomon, H. J., paper presented at the ACS Meeting, Washington, D.C., Sept 1971.

(20) Tsekhanskaya, Y. V.; Iomtev, M. B.; Muskina, E. V. *Zh. Fiz. Khim.* **1964**, *38*, 2166.

(21) Tsekhanskaya, Y. V.; Iomtev, M. B.; Muskina, E. V. *Russ. J. Phys. Chem.* (*Engl. Transl.*) **1962**, *36*, 1177.

(22) Van Gunst, Dissertation, Delft, 1950.

(23) Van Nieuwenburg, C. J.; Van Zon, P. M. *Recl. Trav. Chim. Pays-Bas* **1935**, *54*, 129.

(24) Vitzthum. O.; Hubert, P. German Patent 2 357 590, 1975.

Received for review May 19, 1980. Accepted August 7, 1980. We thank the National Science Foundation for financial support. One of us (R.T.K.) is grateful to the Nestle Co. for financial support in the form of a fellowship.

Critical Mixing of Decyl Alcohol with Dipolar Liquids

Helena Majgier-Baranowska

Research and Development Centre of Television Engineering, Warsaw, Poland

Wiesław Pyżuk*

Department of Chemistry, University of Warsaw, 02-089 Warsaw, Al. Zwirki i Wigury 101, Poland

Wojciech Jeute

Research and Development Centre of Television Engineering, Warsaw, Poland

Jerzy Ziolo

Institute of Physics, Silesian University, Katowice, Poland

The liquid–liquid coexistence curves for critical systems of decanol with five compounds covering a wide range of electric permittivity were determined and analyzed.

Introduction

Investigations of precritical phenomena which occur in the vicinity of the critical solubility point in binary systems call for mixtures with specific properties, e.g., with matched indexes

0021-9568/81/1726-0051$01.00/0 © 1981 American Chemical Society